

## Supporting Information†

### Heterostructure NiO/Ce<sub>1-x</sub>Ni<sub>x</sub>O<sub>2</sub>: Synthesis and synergistic effect of simultaneous surface modification and internal doping for creating superior catalytic performance

*Xin Liu, Ying Zuo, Liping Li, Xinsong Huang, and Guangshe Li\**

†State Key Lab of Structural Chemistry, Fujian Institute of Research on the Structure of Matter, Chinese Academy of Sciences, Fuzhou 350002, P.R. China.

E-mail: guangshe@fjirsm.ac.cn; Fax: +86-591-83702122

#### Sample characterization

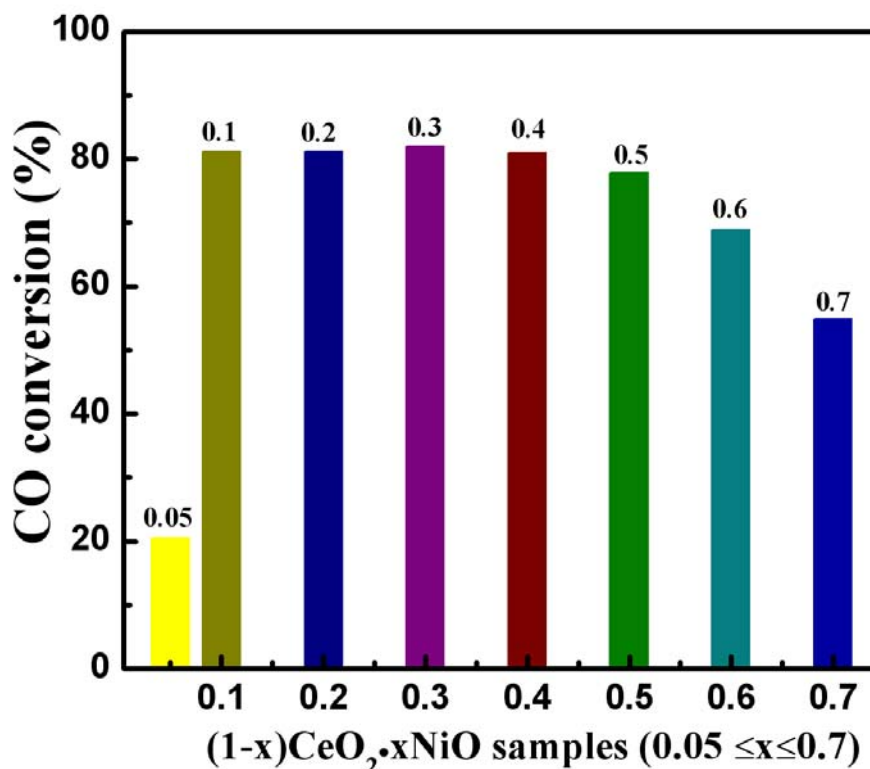


**Fig.S1** CO oxidation activities at 150 °C (reaction temperature) of the samples (1-x) CeO<sub>2</sub>·xNiO (0.05≤x≤0.7) after calcination at 600 °C.

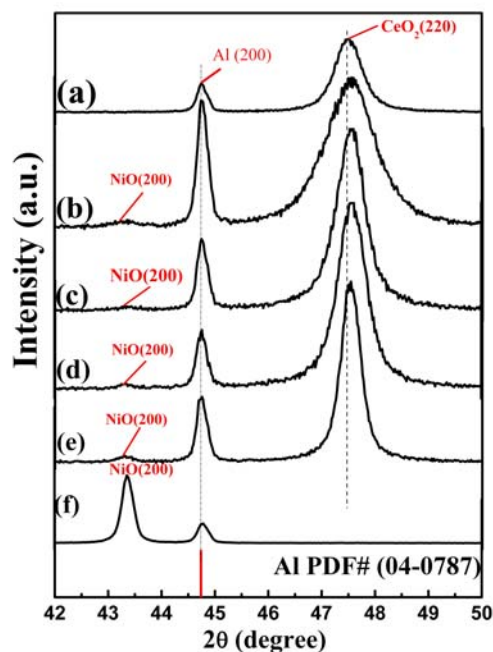


**Fig.S2** an amplified XRD patterns of the samples  $(1-x)\text{CeO}_2 \cdot x\text{NiO}$ , (a) at  $x=0$  after calcination at  $600^\circ\text{C}$ ,  $x=0.1$  after calcinations at (b)  $400^\circ\text{C}$ , (c)  $500^\circ\text{C}$ , (d)  $600^\circ\text{C}$ , (e)  $700^\circ\text{C}$ , and (f)  $x=1$  after calcination at  $600^\circ\text{C}$  from  $42$  to  $50$  degree. Al was selected as an internal standard for peak position calibration.

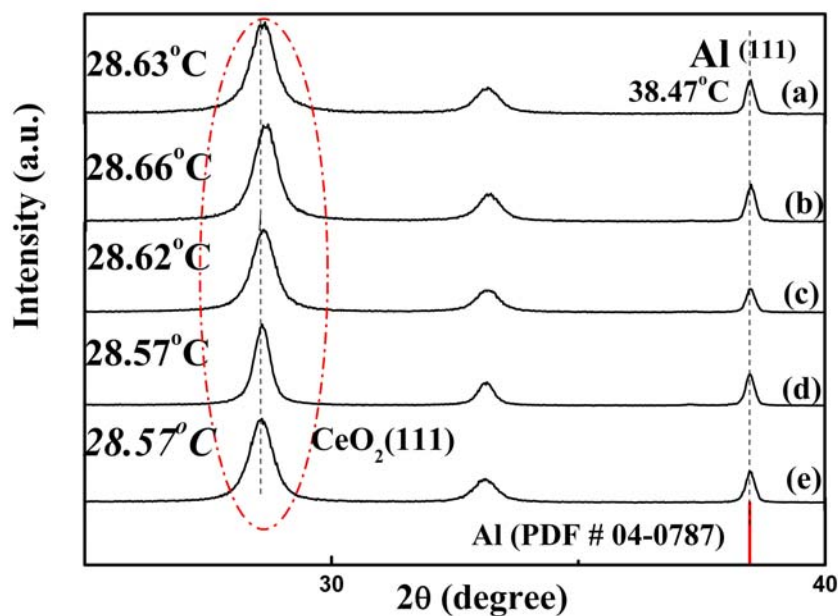


**Fig. S3** Amplified XRD patterns about  $\text{CeO}_2(111)$  crystalline plane patterns of the samples  $(1-x)\text{CeO}_2 \cdot x\text{NiO}$  for  $x=0.1$  after calcinations at (a)  $400^\circ\text{C}$ , (b)  $500^\circ\text{C}$ , (c)  $600^\circ\text{C}$ , (d)  $700^\circ\text{C}$  and (e)  $x=0$  after calcination at  $600^\circ\text{C}$ . Al was selected as an internal standard for peak position calibration.

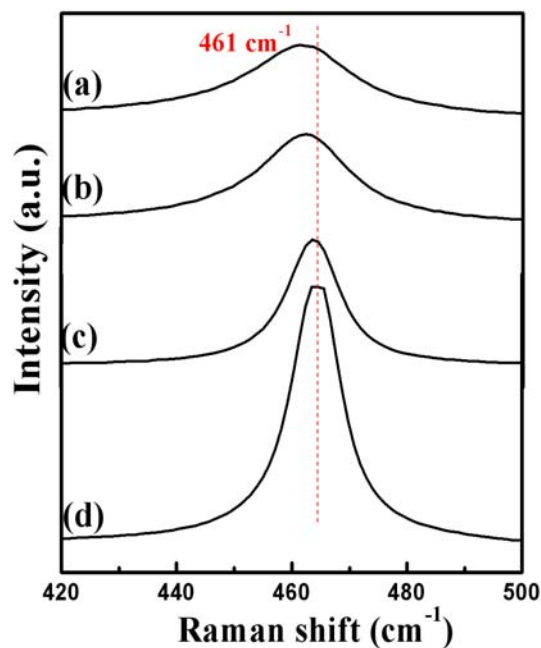


**Fig. S4** Amplified Raman spectrum over a frequency range from 420 to 500 cm<sup>-1</sup> for the samples (1-x) CeO<sub>2</sub>·xNiO at x=0.1 after calcinations at (a) 400, (b) 500, and (c) 700 °C, and (d) at x=0 after calcination at 600 °C.

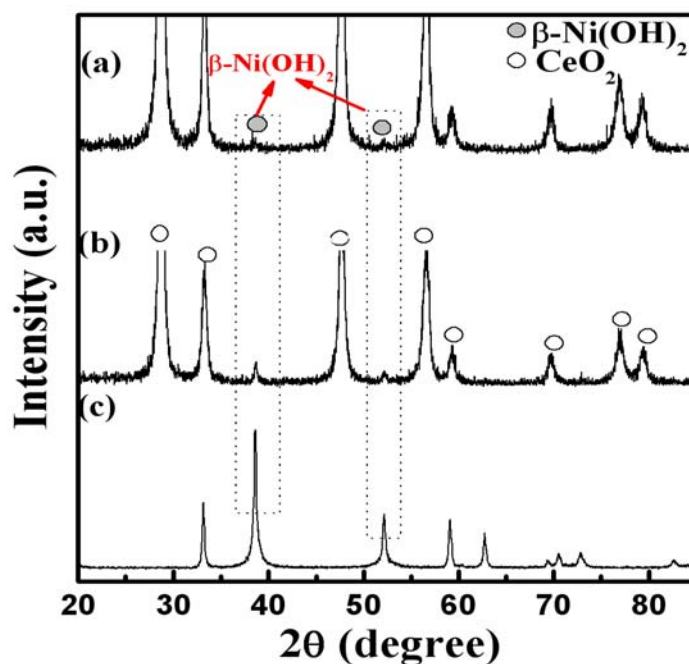


**Fig.S5** Amplified XRD patterns of the sample (1-x)CeO<sub>2</sub>·xNiO at (a) x=0.1, (b) x=0.2, and (c) x=1 before calcinations.

Fig. S5 shows the XRD patterns of the samples (1-x)CeO<sub>2</sub>·xNiO (x=0.1, 0.2, 1) before calcination prepared by hydrothermal method. For further confirm phase composition of the (1-x)CeO<sub>2</sub>·xNiO (x=0.1) catalyst before calcination, the XRD results of (1-x)

$\text{CeO}_2 \cdot x\text{NiO}$  ( $x=0.2, 1$ ) samples are together presented as reference. The diffraction peaks of only  $\beta\text{-Ni(OH)}_2$  (space group P-3m1, JCPDS, No.14-0117) were observed for  $(1-x)\text{CeO}_2 \cdot x\text{NiO}$  ( $x=1$ ) sample before calcination. For  $x=0.1$  and  $0.2$ , it is found that strong diffraction peaks are attributed to  $\text{CeO}_2$  (space group Fm-3m, JCPDS, No.65-5923) and another two weak diffraction peaks presented in XRD patterns are attributed to  $\beta\text{-Ni(OH)}_2$ , the peaks position of which is consistent with pure  $(1-x)\text{CeO}_2 \cdot x\text{NiO}$  ( $x=1$ ). The intensity of  $\beta\text{-Ni(OH)}_2$  is increasing with Ni content.

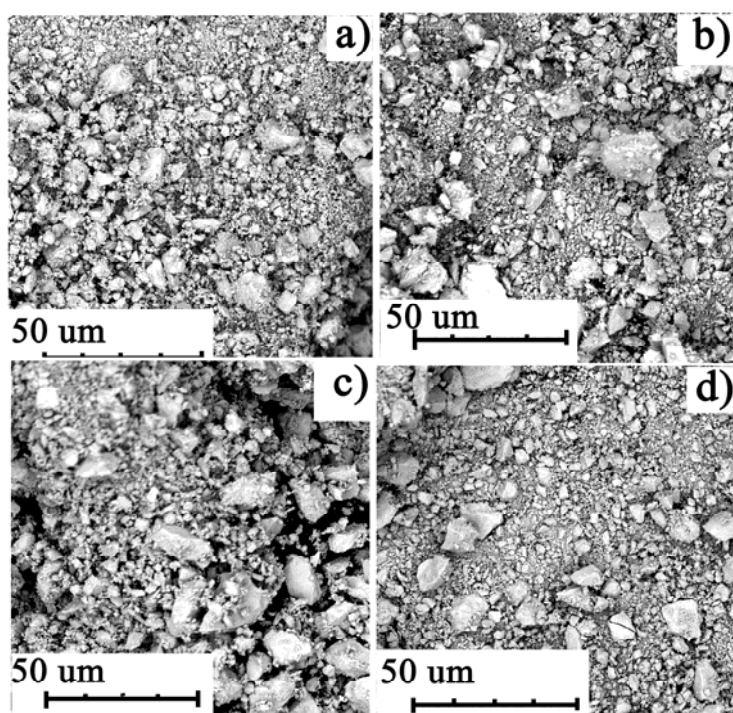


**Fig.S6** SEM micrographs of the sample  $(1-x)\text{CeO}_2 \cdot x\text{NiO}$  prepared at  $x=0.1$  after calcination at (a) 400, (b) 500, (c) 600, and 700 °C.

From the SEM images of Fig. S6, it can be seen that the shape of  $(1-x)\text{CeO}_2 \cdot x\text{NiO}$  sample ( $x=0.1$ ) after calcination is irregular, which is caused by small nanoparticle aggregation after calcination treatment. With the increment of calcination temperature, more nanoparticles aggregate into the bulk together.

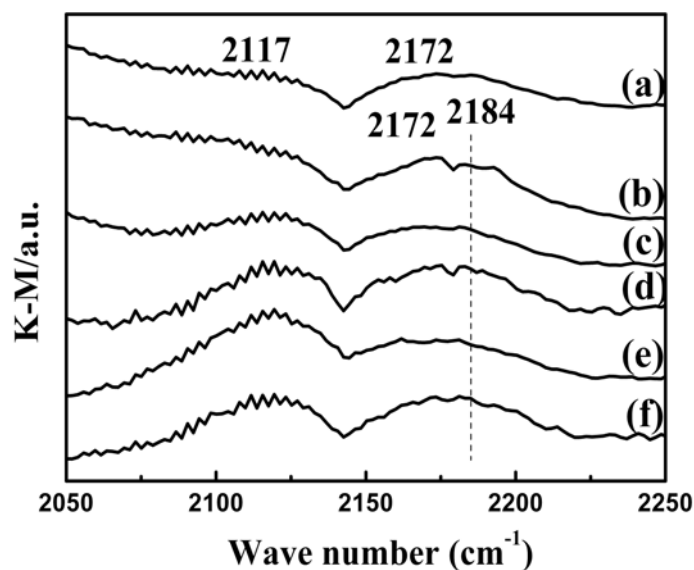


Fig.S7. In-situ DRIFT spectra 2050-2250  $\text{cm}^{-1}$  of  $(1-x)\text{CeO}_2 \cdot x\text{NiO}$  catalysts was exposed to 1% CO/He at  $160^\circ\text{C}$  at (a)  $x=0$  after calcination at  $600^\circ\text{C}$ . (b)  $x=1$  after calcination at  $600^\circ\text{C}$ ,  $x=0.1$  after calcinations at (c)  $400^\circ\text{C}$ , (d)  $500^\circ\text{C}$ , (e)  $600^\circ\text{C}$ , (f)  $700^\circ\text{C}$

The In-situ DRIFT spectra obtained upon exposure of the  $(1-x)\text{CeO}_2 \cdot x\text{NiO}$  catalysts to 1% CO/He gas stream at  $160^\circ\text{C}$  were shown in Fig.S7. The twin bands at 2117 and  $2172 \text{ cm}^{-1}$  are resulted from the P-branch and R-branch of gaseous CO.<sup>[1]</sup> As shown in Fig.S7b, for pure NiO, the band at  $2182 \text{ cm}^{-1}$  is attributed to CO adsorbed on nickel species.<sup>[2]</sup> For the samples at  $x=0.1$  calcined at different temperatures, since the amount of surface NiO is less, it is difficult to observe CO adsorption on Ni species as calcination temperature increases.

- [1] M. Meng, Y. Liu, Z. Sun, L. Zhang and X. Wang, International Journal of Hydrogen Energy, 2012, 37, 14133-14142.
- [2] X. Cheng, A. Zhu, Y. Zhang, Y. Wang, C. T. Au and C. Shi, Applied Catalysis B: Environmental, 2009, 90, 395-404.

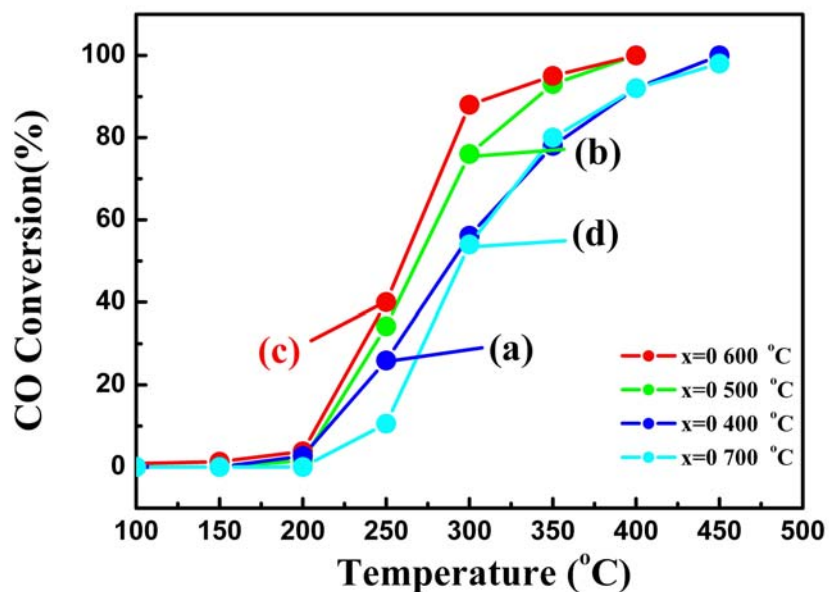


Fig.S8 CO oxidation activities of the samples (1-x)CeO<sub>2</sub>·xNiO for x=0 after calcination at (a) 400 °C (b) 500 °C (c) 600 °C and (d) 700 °C.

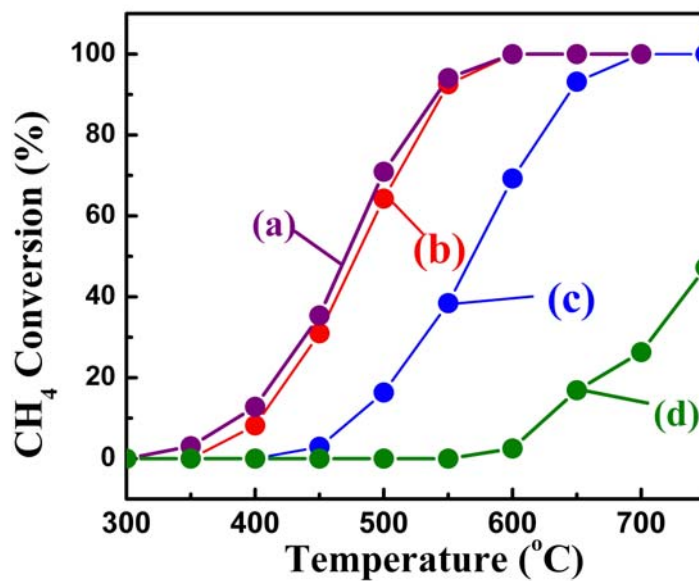


Fig.S9 CH<sub>4</sub> oxidation activities of the samples (1-x)CeO<sub>2</sub>·xNiO for x=0.1 after calcination at (a) 400 °C (b) 500 °C (c) 600 °C and (d) 700 °C.